Local and regional contributions to fine particulate matter in the 18 cities of Sichuan Basin, southwestern China

Xue Qiao[1,2], Hao Guo[2], Ya Tang[3], Pengfei Wang[2], Wenye Deng[4], Xing Zhao[5], Jianlin Hu[6], Qi Ying[7,*], Hongliang Zhang[2,*]

[1]Institute of New Energy and Low-carbon Technology & Healthy Food Evaluation Research Center, Sichuan University, No. 24, South Section One, First Ring Road, Chengdu, Sichuan 610065, China

[2]Department of Civil and Environmental Engineering, Louisiana State University, Baton Rouge LA 70803, USA

[3]College of Architecture and Environment & Healthy Food Evaluation Research Center, Sichuan University, Chengdu 610065, China

[4]Xinjiang Academy of Environmental Protection Science, Urumqi 830011, China

[5]Department of Epidemiology and Biostatistics, West China School of Public Health, Sichuan University, No. 17, Section 3, South Renmin Road, Chengdu, Sichuan 610041, China

[6]Jiangsu Key Laboratory of Atmospheric Environment Monitoring and Pollution Control, Jiangsu Engineering Technology Research Center of Environmental Cleaning Materials, Nanjing University of Information Science & Technology, Nanjing 210044, China

[7]Zachry Department of Civil Engineering, Texas A&M University, College Station, TX 77843, USA

*Corresponding authors: Qi Ying, qying@civil.tamu.edu; Hongliang Zhang, hlzhang@lsu.edu.

Abstract

The Sichuan Basin (SCB) is one of the regions suffering from severe air pollution in China, but fewer studies have been conducted for this region than for the more developed regions in East and North China. In this study, a source-oriented version of the Community Multi-scale Air Quality (CMAQ) model was used to quantify contributions from nine regions to $PM_{2.5}$ (i.e., particulate matter (PM) with an aerodynamic diameter less than 2.5 μm) and its components in the 18 cities within the SCB in the winter (December 2014 to February 2015) and summer (June to August, 2015). In the winter, citywide average $PM_{2.5}$ concentrations are 45~126 μg m^{-3}, with 21~51% and 39~66% due to local and non-local emissions, respectively. In the summer, 15~45% and 25~52% of citywide average $PM_{2.5}$ (14~31 μg m^{-3}) are due to local and non-local emissions, respectively. Compared to primary PM (PPM), the inter-region transport of secondary inorganic aerosols (SIA, including ammonia, nitrate, and sulfate ions (NH_4^+, NO_3^-, and SO_4^{2-}, respectively)) and their gas-phase precursors are greater. The region to the east of SCB (R7, including the central and eastern China and others) is the largest contributor outside the SCB, and it can contribute approximately 80% of $PM_{2.5}$ in the eastern, northeastern, and southeastern rims of the SCB, but only 10% in other SCB regions in both seasons. Under favorable transport conditions, regional transport of air pollutants from R7 could account for up to 35~100 μg m^{-3} of $PM_{2.5}$ in each of the SCB cities in the winter. This study demonstrates that it is important to have joint emission control efforts among cities within the SCB and regions to the east in order to reduce $PM_{2.5}$ concentrations and prevent high $PM_{2.5}$ days for the entire basin.

Keywords: Sichuan Basin, local emission, regional transport, $PM_{2.5}$, source apportionment

1. Introduction

Particulate matter (PM) is one of the major air pollutants in China, including primary and secondary components. Primary PM (PPM) is directly released from emission sources, while secondary PM is formed from their precursors, such as sulfur dioxides (SO_2), nitrogen oxides (NO_x), and ammonia (NH_3). All of them are released from local sources or transported for a long distance (Ying et al., 2014; Zhao et al., 2018). The relative contributions of secondary components to total $PM_{2.5}$ (PM with an aerodynamic diameter less than 2.5 μm) usually increases as $PM_{2.5}$ concentration elevates in megacities (Huang et al., 2014; Qiao et al., 2018).

Air pollution in major economic centers in China, including the North China Plain (NCP), Yangtze River Delta (YRD), and Pearl River Delta (PRD), has been extensively studied in recent years. Regional transport of air pollutants has been identified an important source of PM in the three regions, particularly the precursors of secondary PM (Zhang et al., 2013; Zhao et al., 2013a; Ying et al., 2014; Jiang et al., 2015; Li et al., 2015; Wang et al., 2015; Zheng et al., 2015; Tang et al., 2016; Yang et al., 2018). Several urbanized areas in western China also have been suffering from air pollution due to rapid industrial and urban development, but fewer studies have been conducted compared with the NCP, YRD, and PRD. One such area is the Sichuan Basin (SCB), which covers an area about 0.22 million km^2 and is home to more than 100 million residents in 18 cities, among which Chengdu and Chongqing are the largest two cities in western China (National Bureau of Statistics of China (NBSC), 2015; Table S1). The SCB is topographically isolated, with mountains or plateaus on all sides. They are the Qinghai-Tibetan Plateau (QTP), Yunnan-Guizhou Plateau (YGP), Wushan Mountains (WUM), and Dabashan Mountains (DBM) to the west, south, east, and north of the SCB, respectively. As a result of the basin topography, emissions released from the SCB tend to accumulate in the basin, causing severe air pollution (Ning et al., 2018a; Zhao et al., 2018). In addition, east and central China, which are to the east of the SCB, have considerable contributions to $PM_{2.5}$ for the SCB. For example, Ying (2014) predicted that central and east China had a combined contribution of 29.6% to the total mass of NO_3^- and SO_4^{2-} for Chongqing in January 2009. Due to high emissions within the basin and deep basin landform, annual average concentrations of $PM_{2.5}$ in the SCB were similar to that of NCP and Central China (Figure S1). Annual $PM_{2.5}$ measured in Chengdu and Chongqing in 2015 were 64 and 57 μg m^{-3}, respectively, about six times the World Health Organization (WHO) guideline (10 μg m^{-3}) (WHO, 2006; NBSC, 2015).

To design effective $PM_{2.5}$ control strategies for the SCB, it is necessary to quantify the source contributions and inter-/intra-region transport of $PM_{2.5}$ and its precursors within the SCB and its surrounding regions. There are many types of source apportionment methods, such as receptor-based models, air parcel trajectory models, remote sensing, and chemical transport models (CTMs). Receptor-based models, such as the Positive Matrix Factorization (PMF) (Paatero and Tapper, 1994; Qiu et al., 2019), the Chemical Mass Balance (CMB) (Watson et al., 1990) and a local contribution model proposed by Zhao et. al. (2019), are semi-quantitative and cannot quantitatively determine the source contributions from an exact emission sector or a specific location. They also require a large number of monitoring data and can only resolve source contributions at the monitoring sites (Hopke, 2016). Remote sensing and air parcel trajectory models, such as the Potential Source Contribution Function (PSCF) and the Hybrid Single Particle Lagrangian Integrated Trajectory Model (HYSPLIT) can just reflect the atmospheric dynamics so they are not quantitative for source apportionment of secondary species (Begum et al., 2005; Uno et al., 2009; Stein et al., 2015; Liu et al., 2018; Wu et al., 2018). Compared to above methods, CTMs are more quantitative, as they can be track the source contributions to both primary and secondary air pollutants from a specific region or sectorial source for studies at the local, regional, or global scales (Bove et al., 2014; Kim et al., 2015; Lelieveld et al., 2015; Itahashi et al., 2017; Shi et al., 2017). In CTMs, source contributions are quantified through two methods, namely, sensitivity analysis and tagged-tracer methods (Burr and Zhang, 2011). Sensitivity analysis such as the brute-force method is more suitable to estimate air quality changes due to emission perturbations, as emissions from certain sources would be eliminated or reduced in each simulation of sensitivity analysis (Burr and Zhang, 2011; Han et al., 2018; Huang et al., 2018). In the tagged-tracer method, source-tagged-species are used to track air pollutants from specific emission regions and sectors and they would go through all the non-linear chemical and physical processes in the model, thus this method is considered to provide more realistic evaluations of the contributions of different source sectors or source regions to the current level of air pollution under the current emission intensities (Wang et al., 2009; Burr and Zhang, 2011; Chen et al., 2017).

Transport of $PM_{2.5}$ and its precursors has been studied for Chengdu, Chongqing, and the entire SCB region (Zhu et al., 2018). Based on in-situ observations and the HYSPLIT model, studies have found that dust storms from northwestern China and biomass burning activities would cause high PM days in the two cities, particularly in spring (Zhao et al., 2010; Tao et al., 2013; Chen and Xie, 2014; Chen et al., 2015). Using the PSCF model, a study reported that the main potential sources of $PM_{2.5}$ for Chengdu were from southeastern cities and the western margin of the SCB in addition to local emissions from December 2013 to February 2014 (Liao et al., 2017). Based on the HYSPLIT and PSCF analyses, air pollution was determined mainly from the south during persistent extreme haze days in Chengdu from 6^{th} to 16^{th} January 2015 (Li et al., 2017). However, the aforementioned studies based on the HYSPLIT and PSCF models are not quantitative in terms of emission contributions. Their accuracy is also limited by the meteorological inputs to drive these models, which are often in very coarse resolutions (0.5 to 1.0 degree) that are not enough to accurately predict air pollutant transport within the SCB, as meteorological conditions and pollutant concentrations may vary greatly within short distance (Shi et al., 2017). Also, previous country-level modeling study did not have sufficient spatial resolution to properly quantify the transport among cities within the SCB.

Since both inter-regional transport within the cities in the basin and from outside the region can greatly affect $PM_{2.5}$ concentrations in the 18 SCB cities, systematically quantifying contributions from different regions to $PM_{2.5}$ for all the 18 cities in the SCB is urgently needed as emission controls are further tightened to improve air quality in this region. In this study, an improved source-oriented community multi-scale air quality (CMAQ) model was used to quantify the contributions from nine regions (five within the SCB and four outside) to $PM_{2.5}$ and its components for the 18 SCB cities. The assumption is that the transport of air pollutants is evident among the SCB cities and some cities in the rims of the SCB are greatly affected by emissions outside SCB. Therefore, the objectives of this study are to quantitatively determine (1) the inter-region transport of air pollutants emitted in the SCB and its contributions to $PM_{2.5}$ in the 18 SCB cities and (2) the contributions of emissions outside the basin to $PM_{2.5}$ in the SCB. In this study, the percentage contributions and maximum mass contributions from each region to $PM_{2.5}$ in each city are both presented to better understand the extent of air pollutant transport. We modeled $PM_{2.5}$ and its source contributions only for two seasons, as $PM_{2.5}$ concentrations in the SCB are highest in winter and summer, respectively (Ning et al., 2018a).

2. Methods and materials

2.1. Model description

The source-oriented CMAQ model used in this study is based on the CMAQ model version 5.0.1. The gas phase and aerosol mechanisms are extended from the standard SAPRC-99 photochemical mechanism and aerosol module version 6 (AERO6). This version of the source-oriented CMAQ is capable of simultaneously tracking both primary particulate matter (PPM) and secondary inorganic aerosols (SIA, including NH_4^+, NO_3^-, and SO_4^{2-}) from multiple source sectors and regions. It unifies the two previous models individually developed for PPM (Hu et al., 2015) and SIA (Ying et al., 2014; Shi et al., 2017) into a single consistent model framework. For SIA, multiple source-tagged reactive species are introduced in both gas and particle phases to represent the same species originated from different source sectors or regions. The corresponding photochemical mechanisms, aerosol and cloud modules are expanded so that SIA and their precursors from different regions can be tracked separately throughout the model calculations. For example, NO_2_S1 and NH_3_S2 can be used to represent NO_2 from region 1 and NH_3 from region 2, respectively. After the photochemical mechanism is expanded, the source-tagged species are allowed to go through all processed to form (NH_4_S2)(NO_3_S1) based on additional reactions of $NO_2 + OH \rightarrow HNO_3$ and $NH_3 + HNO_3 \rightarrow NH_4NO_3$. Thus, the contributions of region 1 to NO_3^- and region 2 to NH_4^+ are quantified. For PPM, source-tagged non-reactive tracers are added to track the total amount of PPM emitted from different source sectors and regions. SOA is included in the current model but its source contributions are not resolved.

2.2. Model application

The source-oriented CMAQ model was applied to quantify nine source-region contributions to $PM_{2.5}$ and its components (PPM and SIA) for the 18 cities in the winter (from December 2014 to February 2015) and summer (June to August 2015) using nested domain settings. The locations of domains, nine source-regions, and the 18 cities of the SCB are shown in Figure 1. The horizontal resolutions of the parent and nested domains are 36-km and 12-km, respectively. There are 18 vertical layers with an overall height of 20 km and the layer closest to the land surface is up to 35 m. The geographical regions of emissions are classified into nine source-regions. As Chengdu and Chongqing are the two largest cities in western China and within the SCB, we classified Chengdu, eastern Chongqing, and western Chongqing into three individual regions (R4, R5, and R1, respectively). Western Chongqing is well urbanized and eastern Chongqing is mostly rural areas. The five cities in the northeastern SCB (Bazhong, Dazhou, Guangyuan, Guang'an, and Nanchong) are grouped into R2, as they have relatively lower anthropogenic emission densities compared to most of the other SCB cities and they are located in the upwind areas within the SCB (Qiao et al., 2019). The rest SCB cities are grouped into R3. Sichuan Province excluding those cities within the SCB is R8, most of which remote rural areas. R6 includes three provinces to the south of the SCB and R7 has the Chinese provinces to the east and northeast of the SCB. R9 includes the other jurisdictions to the west of the SCB, including Xinjiang, Qinghai, Gansu, Tibet, and other countries.

Meteorological inputs were generated using the Weather Research and Forecasting (WRF) model version 3.9 based on the 6-hourly FNL (Final) Operational Global Analysis data from the National Center for Atmospheric Research (NCAR) with a spatial resolution of 1.0×1.0^{o} (http://dss.ucar.edu/datasets/ds083.2/). The anthropogenic emission inventory used was the Emission Database for Global Atmospheric Research (EDGAR) version 4.3.1 for the year of 2012 (Crippa et al., 2018). The inventory was directly used for the model year of 2014-2015 as no reliable sources for emission changes in the SCB are available. The monthly EDGAR inventories have a spatial resolution of $0.1^{\circ}\times0.1^{\circ}$ (~10 km×10 km) and were re-projected to the model domains using the Spatial Allocator (https://www.cmascenter.org/sa-tools/). Temporal profiles specific to sources were used to allocate the monthly emission rates to hourly values for CMAQ modeling (Olivier et al., 2003; Streets et al., 2003; Wang et al., 2010). The EDGAR inventory includes carbon monoxide (CO), NO_x, SO_2, NH_3, non-methane volatile organic compounds (NMVOCs), $PM_{2.5}$, PM_{10} (PM with an aerodynamic diameter less than 10 μm), elemental carbon (EC), and organic carbon (OC) from various sources. Emission sources are grouped into six categories: energy, industries, residential activities, on-road transportation, off-road transportation, and agriculture. In addition to these six anthropogenic sources, contributions of biogenic sources were also determined using emissions generated by the Emissions of Gases and Aerosols from Nature (MEGAN) model version 2.1 (Guenther et al., 2012). The emissions from open burning were estimated based on the Fire Inventory from the National Center for Atmospheric Research (NCAR FINN) (Wiedinmyer et al., 2010). Contributions of windblown dust and sea salt emissions were determined based on in-line generated emissions during CMAQ simulations. It should be noted that the uncertainties in emission inventories potentially lead to uncertainties in the contributions.

The initial and boundary conditions (ICs and BCs, respectively) for the 36-km domain were based on CMAQ default profiles, and those for the 12-km domain were generated using the CMAQ outputs from the 36-km simulations. More details about the setup and configurations of the WRF/CMAQ modeling system can be found in a previous publication for China (Kang et al., 2016).

3. Results and discussion

3.1. Model performance

The model performance on meteorological parameters and 24-hr $PM_{2.5}$ in the 12-km domain for the two seasons has been evaluated in a companion paper (Qiao et al., 2019) and is briefly summarized here (Figure S2). As the predictions on wind speed (WS) and wind direction (WD) are important in modeling air pollutant transport (Zhao et al., 2009), the WRF model performance on WS, WD, ambient air temperature (T), and relative humidity (RH) were evaluated by using hourly observations at China's national meteorological stations and the observation data that were downloaded from the National Climate Data Center (NCDC; ftp://ftp.ncdc.noaa.gov/pub/data/noaa/, last accessed on June 20, 2018). The mean biases (MBs) of predicted RH (-10.8% to -1.1%) and T (-0.9 to -0.1˚C) in each month are comparable to other studies in China (Wang et al., 2010; Zhao et al., 2013b; Wang et al., 2013). The MB of WD in each month (-5˚ to 6˚) meet the benchmark of <±10˚ suggested by Emery et al. (2001). Although the MB of WS in each month (0.5 to 1.1 m s^{-1}) does not meet the benchmark of <±0.5 m s^{-1}, the gross errors (GEs: 1.4-1.9 m s^{-1}) are within the benchmark of 2.0 m s^{-1}. For 24-hr $PM_{2.5}$ concentrations, the statistical metrics of model performance are generally within the criteria recommended by Emery et al. (2017) for regulatory applications, with only a few cities exceeding the normalized mean bias (NMB) criteria of <±30% in the winter (Chongqing 42%; Guangyuan 41%; Mianyang 37%; Meishan 31%; Ziyang 48%) and in the summer (Dazhou -39%) (Figure S2). The 24-hr $PM_{2.5}$ predictions meet the goals of normalized mean error (NME<±35%), fractional bias (FB<±30%), and fractional error (FE<±50%) in all the cities in both seasons, except for the NME of Ziyang (58%) in the winter. The predictions of major $PM_{2.5}$ components (including OC, EC, NH_4^+, NO_3^-, and SO_4^{2-}) in Chengdu and Chongqing are comparable with observations, and both predictions and observations suggest that OC and SIA are the largest contributors to $PM_{2.5}$ in summer and winter, with combined contributions about 70% (Qiao et al., 2019).

3.2. Seasonal average contributions

3.2.1. Source contributions at the city centers

In each city, there are 4 to 17 national air quality stations (NAQs), and almost all the NAQs are located in the urban areas, where population densities are higher. Thus, coordinates of the NAQs in the urban area of a given city were averaged to define the city center in order to understand $PM_{2.5}$ concentrations and its sources for the most-populated region of each city. The predicted $PM_{2.5}$ concentrations and source-region contributions at the 18 SCB city centers are presented in Table 1 for winter and Table S2 for summer. In all the city centers, the predicted $PM_{2.5}$ concentrations are much higher in the winter (60~191 μg m^{-3}) than in the summer (14~64 μg m^{-3}). The city centers are considerably affected by both local and regional emissions in both seasons. Emissions within the SCB are the major contributor to $PM_{2.5}$ in Chengdu and Chongqing in both seasons (~80%) and emissions outside the SCB contribute approximately 7~15%. Among the regions within the SCB, local emissions (i.e., emissions from the region where the city center is located) are the largest contributor to $PM_{2.5}$ in Chongqing and Chengdu in both seasons (about 70% and 58%, respectively). However, emissions from R3 (i.e., the 11 cities in the northwestern, western, and southwestern SCB) also have considerable contributions in Chengdu (~20% and 14% in the winter and summer, respectively). For the R3 cities, the contributions of emissions within the SCB (64~83%) are also larger than that from outside the SCB (8~26%) in both seasons. Local emissions are the largest contributor for R3 cities (40~60%), except that Suining has only ~13% due to its local region. The low local contribution in Suining might be because it is less economically developed compared to other cities, except for Bazhong, Guangyuan, and Ya'an, as suggested by the 2015 gross domestic production (GDP; Table S1). For the five cities in the northern SCB (R2), emissions within the SCB account for 40~70% in both seasons, including 37~57% from local emissions. Emissions outside the SCB also have large contributions to the R2 cities (21~36% and 17~28% in the winter and summer, respectively), as R2 is located in one of the regions where winds from R7 intrude the basin (Figure 2a). In the winter, contributions from SOA and others (including IC, BC, windblown dust, and sea salt) are less than 8% each. In the summer, SOA and others each contribute 9~28% and less than 10%, respectively, but the SOA contributions larger than 15% are found only in the city centers where summer $PM_{2.5}$ concentrations are less than 30 $\mu g\ m^{-3}$. In summary, local emissions are the largest contributor for all the city centers in both seasons, except for Suining. The non-local contributions for the city centers are in the ranges of 25~52% in the winter (except for 75% in Suining) and of 14~40% in the summer (except for 61% in Suining), and emissions outside the SCB account for 7~36% in the seasons.

3.2.2. Spatial variations and citywide area-weighted averages

The spatial variations of source-region contributions to $PM_{2.5}$ in the winter and summer are presented in Figures 2 and 3, respectively. In both seasons, local emissions are generally the largest contributor in each city, except that R7 has contributions similar to or larger than that of local emissions for most regions in eastern Chongqing (R5) and R2. Specifically, the contributions from R7 to $PM_{2.5}$ in R2 and R5 are approximately 20~80% in the winter and 20~60% in the summer. R7 also has contributions larger than 20% for a few areas in R3. The regions of R6, R8, and R9 outside the SCB each has contributions of <5% across the basin, except for some very limited areas in the western and southern rims of the SCB. The contributions from R6, R8, and R9 are low because these areas are less urbanized and industrialized. In addition, the mountains to the west and south of the SCB also prevent the transport of air pollutants from these regions into the SCB (Figures 1c, 2a, and 3a). In summary, R7 is the sole non-SCB region that can have >20% contributions to $PM_{2.5}$ in the SCB, and its impact decreases from the northeast, east, and southeast to others in the basin.

As shown in Figures 2 and 3, $PM_{2.5}$ concentrations and its source contributions from a given region may vary greatly within a city in both seasons. For example, about 20~80% of $PM_{2.5}$ across

Chengdu (R4) and western Chongqing (R1) are due to local emissions in each season, and higher $PM_{2.5}$ concentrations are generally related to higher local contributions. For the downwind regions of Chengdu and western Chongqing, they receive considerable contributions from the two mega-cities. For example, over half areas of Meishan and Ya'an, which are downwind of Chengdu, have 20~40% and 20~60% of $PM_{2.5}$ concentrations due to Chengdu in the winter, respectively. In the two seasons, western Chongqing contributes to about 10~40% of $PM_{2.5}$ concentrations in its neighboring cities, except that most area of eastern Chongqing (R5) is not affected by emissions from western Chongqing, as R5 is upwind of western Chongqing (Figure 2a). Because of the large spatial variations of $PM_{2.5}$ and its source contributions in the basin, we further calculated their citywide area-weighted averages (Table 2). In the winter, the citywide average $PM_{2.5}$ concentrations in Chengdu and urban Chongqing are 99 and 110 μg m^{-3}, with only 38% and 47% due to local emissions, respectively. Non-local emissions also have high contributions in other SCB cities, with citywide averages of 39~66% and 25~52% in the winter and summer, respectively. The above suggests the importance of regional emission control to reduce $PM_{2.5}$ concentrations for the entire basin.

3.2.3. Differences in PPM and SIA

The transport distances of PPM, NH_4^+, NO_3^-, and SO_4^{2-} might be different, because of the differences in chemical and physical processes that affect their concentrations in the atmosphere (Ying et al., 2014; Hu et al., 2015). This leads to significant differences in their regional distributions and thus requires different control strategies. From the source-region contributions to PPM and SIA for each city center shown in Figure 4, it is obvious that the regional transport of SIA is more significant than that of PPM. In the city centers of Chengdu and Chongqing, 55~65% of PPM and 25~45% of SIA are due to local emissions in the two seasons. In the city centers of R2, PPM is also more from local emissions (65~80%) than SIA is (25~45%) in both seasons. Similarly, local emissions have larger contributions to PPM (50~85%) than to SIA (34~50%) in all the city centers of R3 except for Suining, which is not significantly affected by local emissions. The spatial distributions of source-region contributions to PPM and SIA also indicate more significant transport of SIA (Figures S3-6) than PPM. For example, R3 contributes to >20% of SIA across entire Chengdu, but only half areas of Chengdu are about equally affected (>20%) by R3 for PPM. From the north to south in R2, the contributions from R7 to PPM decrease from ~55% to ~10%, while the contributions of R7 to SIA decrease from ~75% to ~20%. The contributions to NH_4^+, NO_3^-, and SO_4^{2-} in each city center from local emissions and emissions within and outside SCB are further analyzed (Tables S3 and S4). In each city center, concentrations of SO_4^{2-} (3.8~12.6 and 12~41 μg m^{-3}) are much higher than that of NH_4^+ (1.4~4.0 and 6.0~17.0 μg m^{-3}) and NO_3^- (0.3~2.4 and 6~20 μg m^{-3}) in the summer and winter, respectively. Also, the transport of SO_4^{2-} and its precursor is greater than the other two ions, as the percentage contributions from emissions outside the SCB to SO_4^{2-} is higher than that to NH_4^+ and NO_3^- in each city center. In both seasons, emissions outside SCB contribute <25% of NH_4^+ in the city centers, except for

Chongqing (26%) in the summer and Bazhong (36%) and Guangyuan (33%) in the winter. As for NO_3^-, emissions outside SCB also contribute <25% in the city centers in both seasons, except for Bazhong (49%), Dazhou (34%), and Guangyuan (25%) in the summer and all the cities of R2 (27~57%) in the winter. In the two seasons, emissions outside SCB account for 22~33% of SO_4^{2-} in Chengdu and Chongqing, while they contribute 52~70% of SO_4^{2-} for the R2 cities. For the R3 cities, emissions outside SCB account for 25~53% of SO_4^{2-} in the city centers in the seasons, except for Meishan (21%) in the winter. All the above suggest that it would be more efficient to control the SIA (particularly SO_4^{2-}) and its precursors than PPM in order to reduce the transport of air pollutants within and into the basin.

3.3. Maximum daily contributions from a given region

The maximum daily contribution from a given region to $PM_{2.5}$ (MDC, μg m^{-3}) in each city center is shown in Table 3 for winter and Table S5 for summer. The largest MDC for each city center (79~291 and 13~147 μg m^{-3} in the winter and summer, respectively) are found associated with local emissions, except for Guangyuan and Suining. In Guangyuan and Suining, the largest MDCs in the winter are from R7 (62 μg m^{-3}) and R2 (110 μg m^{-3}), both are slightly higher than that from the local region of 60 and 105 μg m^{-3}, respectively. Table 3 also shows that the inter-basin transport of air pollutants can have large contributions (>50 μg m^{-3}) on high $PM_{2.5}$ days (>150 μg m^{-3}). For example, R7 contributes 99 μg m^{-3} to total $PM_{2.5}$ (200 μg m^{-3}) in Chongqing on a winter day. In Nanchong, the MDC due to western Chongqing (R1) is 58 μg m^{-3}, when daily $PM_{2.5}$ is 180 μg m^{-3} on that day. In Chengdu, R3 and R7 can contribute up to 86 and 63 μg m^{-3} on the days with daily $PM_{2.5}$ of 267 and 151 μg m^{-3}, respectively. In Deyang and Meishan, the MDCs from Chengdu are 147 and 138 μg m^{-3} on the days having daily $PM_{2.5}$ of 288 and 235 μg m^{-3}, respectively. Table S4 shows that air pollutant regional transport is also significant on certain days in the summer. For example, the highest summer MDC from R7 among the 18 central cities is found for Bazhong (36 μg m^{-3}), when daily $PM_{2.5}$ is 63 μg m^{-3}. Chengdu contributes about 44, 16, 55, 13, 7, and 21 μg m^{-3} to Deyang, Leshan, Meishan, Ya'an, and Mianyang on the summer days, when daily $PM_{2.5}$ are 89, 56, 100, 85, 22, and 54 μg m^{-3}, respectively. All the above suggest that joint effects should be made by neighboring cities and the provinces to the east of the SCB in order to prevent high $PM_{2.5}$ episodes for the SCB.

3.4. Impacts of topography on $PM_{2.5}$ concentrations

While air pollutant emissions are the root of air pollution, topography and meteorological conditions play a very important role on determining the fate of pollutants including dispersion, accumulation, and transformation (Arya, 1999; Zhang et al., 2015; He et al., 2017). It has been widely noticed that heavy air pollution often occurs in well urbanized and/or industrialized cities associated with mountains and basins, such as Beijing, Chengdu, Xi'an, and Lanzhou in China

(Chambers et al., 2015; Bei et al., 2017; Bei et al., 2018; Ning et al. 2018), Mexico City, Salt Lake City, and Los Angeles in the North America (Langford et al., 2010; Witeman et al., 2014; Calderón-Garcidueñas et al., 2015), and megacities in the Mediterranean Basin of the Europe (Kanakidou et al., 2011). The SCB is surrounded by the QTP to the west, YGP to the south, WUM to the east, and DBM to the northeast. Mainly affected by the high elevations of the QTP and YGP, near-surface winds mainly intrude the basin from the north, east, and southeast in the summer and winter, as shown in Figures 2(a) and 3(a). Consequently, R7 is the largest contributor outside the basin, contributing 20~60% of $PM_{2.5}$ in the eastern, northeastern, and southeastern parts of the SCB (Figures 2(h) and 3(h)), where $PM_{2.5}$ concentrations are relatively lower in the SCB (<75 and 25 μg m^{-3} in the winter and summer, respectively). The contributions from R6 (including YGP) and R8 (including QTP) are <10% along the western and southern rims of the SCB. Within the basin, near-surface winds travel anti-clockwise wind and form a cyclone near Yibin, Zigong, Neijiang, and Luzhou in the south (Figures 1(b), 2(a), and 3(a)) (Lin, 2015), causing air pollutants transported to and accumulated at the cyclone. $PM_{2.5}$ concentrations in the cyclone-affected region (mostly 100-150 and 30~50 μg m^{-3} in the winter and summer, respectively) are generally lower than that of Chengdu and Chongqing but are higher than that of most of other regions. In Yibin, Zigong, Neijiang, and Luzhou, at least 39~53% and 25~44% of citywide average $PM_{2.5}$ concentrations are not due to their own emissions in the winter and summer, respectively (Tables 2 and S2). R7 only contributes about 10% to $PM_{2.5}$ in the cyclone-affected region. In order to reduce seasonal and annual concentrations of $PM_{2.5}$ within the SCB, the emissions and inter-city transport of air pollutants within the basin should receive the priorities to be controlled.

4. Conclusion

In this study, a source-oriented CMAQ model was applied to quantify contributions of nine regions to $PM_{2.5}$ for the 18 cities in the SCB. The simulations were carried out for winter (December 2014 to February 2015) and summer (June to August 2015). Predicted citywide area-weighted average $PM_{2.5}$ concentrations are much higher in the winter (60~191 μg m^{-3}) than in the summer (14~64 μg m^{-3}). In the winter, the citywide average $PM_{2.5}$ concentrations in Chengdu and western Chongqing are 99 and 110 μg m^{-3}, with 44% and 52% due to non-local emissions, respectively. Non-local emissions also have high contributions in other SCB cities, with citywide averages of 39~66% and 25~52% in the winter and summer, respectively. Among the four regions outside the SCB, only the one to the northeast, east, and southeast of the SCB (R7) has large contributions to $PM_{2.5}$ concentrations for the SCB in both seasons (10~80%), and the contributions decrease from the rims of the northeastern, eastern, and southeastern SCB to other regions. However, the MDCs from R7 are large (35~99 μg m^{-3}) for all the city centers in the winter. On high $PM_{2.5}$ days in the winter, emissions outside SCB can contribute up to 99 μg m^{-3} in a city center, suggesting the importance of regional emission control in not just reducing averaged $PM_{2.5}$ but also preventing severe PM pollution events. The transport of SIA is greater than that of PPM, suggested by that local emissions have higher contributions to PPM (>55%) than to SIA (<45%)

in the city centers in both seasons. Among the three ions of SIA, the transport of SO_4^{2-} and its gas-phase precursor (SO_2) is the greatest in general, as >50% of it in all the city centers is associated with non-local emissions in both seasons, except that the contributions are 37~44% in Chongqing and Chengdu in the summer and Chongqing in the winter. In conclusion, in order to reduce $PM_{2.5}$ concentrations and prevent high $PM_{2.5}$ days for the entire SCB, local emissions and the transport of air pollutants within and across SCB should be controlled simultaneously.

Author contributions. XQ, YT, and HZ designed research. HG, JH, QY, and HZ contributed to model development and configuration. XQ, HG, PW, WD, and XZ analyzed the data. XQ prepared the manuscript and all co-authors helped improve the manuscript.

Competing interests. The authors declare that they have no conflict of interest.

Acknowledgment. Portions of this research were conducted with high-performance computing resources provided by the Louisiana State University (http://www.hpc.lsu.edu). This study is sponsored by the International Collaboration Project of the Science & Technology Department of Sichuan Province [2017HH0048], the National Natural Science Foundation of China [41628102], the Program of Introducing Talents of Discipline to Universities [B08037], and $PM_{2.5}$ monitoring in the campuses of Sichuan University [SCU2015CC0001], and the Chinese Scholarship Council [201706245007].

References

Arya, S. Pal: Air pollution meteorology and dispersion, Oxford University Press, New York, United States, 1999.

Begum, B. A., Kim, E., Jeong, C.-H., Lee, D. W., and Hopke, P. K.: Evaluation of the potential source contribution function using the 2002 Quebec forest fire episode, Atmos. Environ., 39, 3719-3724, 2005.

Bei, N. F., Zhao, L. N., Wu, J. R.,Li, X., Feng, T., and Li, G. H.: Impacts of sea-land and mountain-valley circulations on the air pollution in Beijing-Tianjin-Hebei (BTH): A case study, Environ. Pollut., 234, 429-438, 2018.

Bei, N. F., Zhao, L. N., Xiao, B., Meng, N., and Feng, T.: Impacts of local circulations on the wintertime air pollution in the Guanzhong Basin, China, Sci. Total Environ., 592, 373-390, 2017.

Bove, M., Brotto, P., Cassola, F., Cuccia, E., Massabò, D., Mazzino, A., Piazzalunga, A., and Prati, P.: An integrated $PM_{2.5}$ source apportionment study: positive matrix factorisation vs. the chemical transport model CAMx, Atmos. Environ., 94, 274-286, 2014.

Burr, M. J., and Zhang, Y.: Source apportionment of fine particulate matter over the Eastern U.S. Part I: source sensitivity simulations using CMAQ with the Brute Force method, Atmos. Pollut. Res., 2, 300-317, https://doi.org/10.5094/APR.2011.036, 2011.

Calderón-Garcidueñas, L., Kulesza, R. J., Doty, R. L., D'Angiulli, A., and Torres-Jardón, R.: Megacities air pollution problems: Mexico City Metropolitan Area critical issues on the central nervous system pediatric impact, Environ. Res., 137, 157-169, 2015.

Chambers, S. D., Wang, F., Williams, A. G., Deng, X. D., Zhang,H., Lonati, G., Crawford, J., Griffiths, A. D., Lanniello, A., and Allegrini, I.: Quantifying the influences of atmospheric stability on air pollution in Lanzhou, China, using a radon-based stability monitor, Atmos. Environ., 107, 233-243, 2015.

Chen, D., Liu, X., Lang, J., Zhou, Y., Wei, L., Wang, X., and Guo, X.: Estimating the contribution of regional transport to $PM_{2.5}$ air pollution in a rural area on the North China Plain, Sci. Total Environ., 583, 280-291, https://doi.org/10.1016/j.scitotenv.2017.01.066, 2017.

Chen, Y., and Xie, S.: Characteristics and formation mechanism of a heavy air pollution episode caused by biomass burning in Chengdu, Southwest China, Sci. Total Environ., 473-474, 507-517, https://doi.org/10.1016/j.scitotenv.2013.12.069, 2014.

Chen, Y., Luo, B., and Xie, S.: Characteristics of the long-range transport dust events in Chengdu, Southwest China, Atmos. Environ., 122, 713-722, 2015.

Crippa, M., Guizzardi, D., Muntean, M., Schaaf, E., Dentener, F., van Aardenne, J. A., Monni, S., Doering, U., Olivier, J. G. J., Pagliari, V., and Janssens-Maenhout, G.: Gridded Emissions of Air Pollutants for the period 1970-2012 within EDGAR v4.3.2, Earth Sys. Sci. Data, 2018, 1-40, 2018.

Emery, C., Tai, E., and Yarwood, G.: Enhanced meteorological modeling and performance evaluation for two Texas ozone episodes. Final report submitted to Texas natural resources conservation commission, prepared by ENVIRON, International Corp., Novato., 2001.

Emery, C., Liu, Z., Russell, A. G., Odman, M. T., Yarwood, G., and Kumar, N.: Recommendations on statistics and benchmarks to assess photochemical model performance, J. Air Waste Manage., 67, 582-598, 2017.

Guenther, A., Jiang, X., Heald, C., Sakulyanontvittaya, T., Duhl, T., Emmons, L., and Wang, X.: The Model of Emissions of Gases and Aerosols from Nature version 2.1 (MEGAN2. 1): an extended and updated framework for modeling biogenic emissions, Geosci. Model Dev., 5, 1471-1492, 2012.

Han, X., Zhu, L., Wang, S., Meng, X., Zhang, M., and Hu, J. L.: Modeling study of impacts on surface ozone of regional transport and emissions reductions over North China Plain in summer 2015, Atmos. Chem. Phys., 18, 12207-12221, 2018.

He, J., Gong, S., Yu, Y., Yu, L. J., Wu, L., Mao, H. J., Song, C. B., Zhao, S. P., Liu, H. L., Li, X. Y., and Li, R. P.: Air pollution characteristics and their relation to meteorological conditions during 2014–2015 in major Chinese cities, Environ. Pollut., 223, 484-496, 2017.

Hopke, P. K.: Review of receptor modeling methods for source apportionment, J. Air Waste Manage., 66, 237-259, 2016.

Hu, J., Wu, L., Zheng, B., Zhang, Q., He, K., Chang, Q., Li, X., Yang, F., Ying, Q., and Zhang, H.: Source contributions and regional transport of primary particulate matter in China, Environ. Pollut., 207, 31-42, 2015.

Huang, Y., Deng, T., Li, Z., Wang, N., Yin, C., Wang, S., and Fan, S.: Numerical simulations for the sources apportionment and control strategies of $PM_{2.5}$ over Pearl River Delta, China, part I: Inventory and $PM_{2.5}$ sources apportionment, Sci. Total Environ., 634, 1631-1644, https://doi.org/10.1016/j.scitotenv.2018.04.208, 2018.

Huang, R. J., Zhang, Y. L., Bozzetti, C., Ho, K. F. Cao, J. J., Han, Y. M., Daellenbach, K. R., Slowik, J. G., Platt, S. M., Canonaco, F., Zotter, P., Wolf, R., Pieber, S. M., Bruns, E. A., Crippa, M., Ciarelli, G., Pizaazlunga, A., Schwikowski, M., Abbaszade, G., Schnelle-Kreis, J., Zimmermann, R., An, Z. S., Szidat, S., Baltensperger, U., Haddad, I. E., Prévôt, A. H.: High secondary aerosol contribution to particulate pollution during haze events in China, Nature, 514, 218-222, 2014.

Itahashi, S., Hayami, H., Yumimoto, K., and Uno, I.: Chinese province-scale source apportionments for sulfate aerosol in 2005 evaluated by the tagged tracer method, Environ. Pollut., 220, 1366-1375, 2017.

Jiang, C., Wang, H., Zhao, T., Li, T., and Che, H.: Modeling study of $PM_{2.5}$ pollutant transport across cities in China's Jing–Jin–Ji region during a severe haze episode in December 2013, Atmos. Chem. Phys., 15, 5803-5814, 2015.

Kanakidou, M., Mihalopoulos, N., Kindap, T., Im, U., Vrekoussis, M., and Gerasopoulos, E. et al.: Megacities as hot spots of air pollution in the East Mediterranean, Atmos. Environ., 45(6), 1223-1235, 2011.

Kang, Y., Liu, M., Song, Y., Huang, X., Yao, H., Cai, X., Zhang, H., Kang, L., Liu, X., and Yan, X.: High-resolution ammonia emissions inventories in China from 1980-2012, Atmos. Chem. Phys., 15, 26959-26995 2016.

Kim, P. S., Jacob, D. J., Fisher, J. A., Travis, K., Yu, K., Zhu, L., Yantosca, R. M., Sulprizio, M., Jimenez, J. L., and Campuzano-Jost, P.: Sources, seasonality, and trends of southeast US aerosol: an integrated analysis of surface, aircraft, and satellite observations with the GEOS-Chem chemical transport model, Atmos. Chem. Phys., 15, 10411-10433, 2015.

Langford, A. O., Senff, C. J., Alvarez, R. J., Banta, R. M., and Hardesty, R. M.: Long-range transport of ozone from the Los Angeles Basin: A case study, Geophys. Res. Lett., 37, L06807, 2010.

Lelieveld, J., Evans, J. S., Fnais, M., Giannadaki, D., and Pozzer, A.: The contribution of outdoor air pollution sources to premature mortality on a global scale, Nature, 525, 367-371, 2015.

Li, L., Tan, Q., Zhang, Y., Feng, M., Qu, Y., An, J., and Liu, X.: Characteristics and source apportionment of $PM_{2.5}$ during persistent extreme haze events in Chengdu, southwest China, Environ. Pollut., 230, 718-729, 2017.

Li, P., Yan, R., Yu, S., Wang, S., Liu, W., and Bao, H.: Reinstate regional transport of $PM_{2.5}$ as a major cause of severe haze in Beijing, PNAS, 112, E2739-E2740, 2015.

Lin, N.: The research on transport law of atmospheric pollutant and joint prevention and control of air pollution technology in Sichuan Province, Southwest Jiaotong University, Chengdu, China, 2015.

Liao, T., Wang, S., Ai, J., Gui, K., Duan, B., Zhao, Q., Zhang, X., Jiang, W., and Sun, Y.: Heavy pollution episodes, transport pathways and potential sources of $PM_{2.5}$ during the winter of 2013 in Chengdu (China), Sci. Total Environ., 584, 1056-1065, 2017.

Liu, S., Hua, S., Wang, K., Qiu, P., Liu, H., Wu, B., Shao, P., Liu, X., Wu, Y., and Xue, Y.: Spatial-temporal variation characteristics of air pollution in Henan of China: Localized emission inventory, WRF/Chem simulations and potential source contribution analysis, Sci. Total Environ., 624, 396-406, 2018.

National Bureau of Statistics (NSBC): China Statistics Yearbook. http://www.stats.gov.cn/tjsj/ndsj/2016/indexch.htm, 2015.

Ning, G., Wang, S., Ma, M., Ni, C., Shang, Z., Wang, J., and Li, J.: Characteristics of air pollution in different zones of Sichuan Basin, China, Sci. Total Environ., 612, 975-984, 2018a.

Ning, G., Wang, S., Yim, S. H. L., Li, J. X., Hu, Y. L., Shang, Z. W., Wang, J. Y., and Wang, J. X.: Impact of low-pressure systems on winter heavy air pollution in the northwest Sichuan Basin, China, Atmos. Chem. Phys., 18(18), 13601-13615, 2018b.

Paatero, P., and Tapper, U.: Positive matrix factorization: A non-negative factor model with optimal utilization of error estimates of data values, Environmetrics, 5, 111-126, 1994.

Qiao, X., Guo, H., Wang, P. F., Tang, Y., Ying, Q., Zhao, X., Deng, W. Y., and Zhang, H. L.: Modeling Fine Particulate Matter and Ozone in the 18 Cities of Sichuan Basin, Southwestern China, Aerosol Air Qual. Res., submitted.

Qiao, X., Ying, Q., Li, X. H., Zhang, H. L., Hu, J. L., Tang, Y., and Chen X.: Source apportionment of PM2.5 for 25 Chinese provincial capitals and municipalities using a source-oriented community multiscale air quality model, Sci. Total Environ., 612, 462-471, 2018.

Qiu, Y.M., Xie, Q. R., Wang, J. F., Xu, W. Q., Li, L. J., Wang, Q. Q., Zhao, J., and Chen, Y. T. et al.: Vertical characterization and source apportionment of water-soluble organic aerosol with high-resolution aerosol mass spectrometry in Beijing, China, ACS Earth Space Chem., 3, 273–284, 2019.

Shi, Z., Li, J., Huang, L., Wang, P., Wu, L., Ying, Q., Zhang, H., Lu, L., Liu, X., Liao, H., and Hu, J.: Source apportionment of fine particulate matter in China in 2013 using a source-oriented chemical transport model, Sci. Total Environ., 601-602, 1476-1487, https://doi.org/10.1016/j.scitotenv.2017.06.019, 2017.

Shi, X, Q., Zhao, C. F., Jiang, J. H., Wang, C. Y., Yang, X., and Yung, Y. L.: Spatial representativeness of PM2.5 concentrations obtained using observations from network stations, J. Geophys. Res-Atm., 123, 2018.

Stein, A., Draxler, R. R., Rolph, G. D., Stunder, B. J., Cohen, M., and Ngan, F.: NOAA's HYSPLIT atmospheric transport and dispersion modeling system, Bull. Amer. Meteor. Soc. , 96, 2059-2077, 2015.

Tang, L., Yu, H., Ding, A., Zhang, Y., Qin, W., Wang, Z., Chen, W., Hua, Y., and Yang, X.: Regional contribution to PM_1 pollution during winter haze in Yangtze River Delta, China, Sci. Total Environ., 541, 161-166, 2016.

Tao, J., Zhang, L., Engling, G., Zhang, R., Yang, Y., Cao, J., Zhu, C., Wang, Q., and Luo, L.: Chemical composition of $PM_{2.5}$ in an urban environment in Chengdu, China: Importance of springtime dust storms and biomass burning, Atmos. Res., 122, 270-283, 2013.

Uno, I., Eguchi, K., Yumimoto, K., Takemura, T., Shimizu, A., Uematsu, M., Liu, Z., Wang, Z., Hara, Y., and Sugimoto, N.: Asian dust transported one full circuit around the globe, Nat. Geosci., 2, 557-560, 2009.

Wang, L., Jang, C., Zhang, Y., Wang, K., Zhang, Q., Streets, D., Fu, J., Lei, Y., Schreifels, J., He, K., Hao, J., Lam, Y. F., Lin, J., Meskhidze, N., Voorhees, S., Evarts, D., and Phillips, S.: Assessment of air quality benefits from national air pollution control policies in China. Part I: Background, emission scenarios and evaluation of meteorological predictions, Atmos. Environ., 44, 3442-3448, https://doi.org/10.1016/j.atmosenv.2010.05.051, 2010.

Wang, L., Wei, Z., Yang, J., Zhang, Y., Zhang, F., Su, J., Meng, C., and Zhang, Q.: The 2013 severe haze over the southern Hebei, China: model evaluation, source apportionment, and policy implications, Atmos. Chem. Phys., 13, 3151-3173, 2013.

Wang, M., Cao, C., Li, G., and Singh, R.: Analysis of a severe prolonged regional haze episode in the Yangtze River Delta, China, Atmos. Environ., 102, 112-121, 2015.

Wang, Z. S., Chao-Jung, C., and Tonnesen, G. S.: Development of a tagged species source apportionment algorithm to characterize three-dimensional transport and transformation of precursors and secondary pollutants, J. Geophys. Res. Atmos., 114, 2009.

Watson, J. G., Robinson, N. F., Chow, J. C., Henry, R. C., Kim, B., Pace, T., Meyer, E. L., and Nguyen, Q.: The USEPA/DRI chemical mass balance receptor model, CMB 7.0, Environ. Softw., 5, 38-49, 1990.

Whiteman, C. D., Hoch, S. W., Horel, J. D., and Charland, A.: Relationship between particulate air pollution and meteorological variables in Utah's Salt Lake Valley, Atmos. Environ., 94, 742-753, 2014.

WHO: WHO air quality guidelines for particulate matter, ozone, nitrogen dioxide and sulfur dioxide. http://apps.who.int/iris/bitstream/handle/10665/69477/WHO_SDE_PHE_OEH_06.02_eng.pdf;sequence=1, 2006.

Wiedinmyer, C., Akagi, S., Yokelson, R., Emmons, L., Al-Saadi, J., Orlando, J., and Soja, A.: The Fire INventory from NCAR (FINN)–a high resolution global model to estimate the emissions from open burning, Geosci. Model Dev., 3, 2439-2476, 2010.

Wu, Y., Arapi, A., Huang, J., Gross, B., and Moshary, F.: Intra-continental wildfire smoke transport and impact on local air quality observed by ground-based and satellite remote sensing in New York City, Atmos. Environ., 187, 266-281, 2018.

Yang, X., Zhao, C., Zhou, L., Li, Z., Cribb, M., and Yang, S.: Wintertime cooling and a potential connection with transported aerosols in Hong Kong during recent decades, Atmos. Res., 211, 52-61, 2018.

Ying, Q., Wu, L., and Zhang, H.: Local and inter-regional contributions to $PM_{2.5}$ nitrate and sulfate in China, Atmos. Environ., 94, 582-592, https://doi.org/10.1016/j.atmosenv.2014.05.078, 2014.

Zhang, H. L., Wang, Y., Hu, J. L., Ying, Q., and Hu, X. M.: Relationships between meteorological parameters and criteria air pollutants in three megacities in China, Environ. Res., 140, 242-254, 2015.

Zhang, R., Jing, J., Tao, J., Hsu, S. C., Wang, G., Cao, J., Lee, C. S. L., Zhu, L., Chen, Z., and Zhao, Y.: Chemical characterization and source apportionment of $PM_{2.5}$ in Beijing: seasonal perspective, Atmos. Chem. Phys., 13, 7053-7074, 2013.

Zhao, B., Wang, S., Dong, X., Wang, J., Duan, L., Fu, X., Hao, J., and Fu, J.: Environmental effects of the recent emission changes in China: implications for particulate matter pollution and soil acidification, Environ. Res. Lett., 8, 024031, 2013b.

Zhao, C., Andrews, A. E., Bianco, L., Eluszkiewicz, J., Hirsch, A., MacDonald, C., Nehrkorn, T., and Fischer, M. L.: Atmospheric inverse estimates of methane emissions from Central California, J. Geophys. Res-Atm., 114, 2009.

Zhao, Q., He, K., Rahn, K., Ma, Y., Jia, Y., Yang, F., Duan, F., Lei, Y., Cheng, Y., and Wang, S.: Dust storms come to Central and Southwestern China, too: implications from a major dust event in Chongqing, Atmos. Chem. Phys., 10, 2615-2630, 2010.

Zhao, C. F., Li, Y. N., Zhang, F., Sun, Y. L., and Wang, P. C.: Growth rates of fine aerosal particles at a site near Beijing in June 2013, Adv. Atmos. SCI., 35, 209-217, 2018.

Zhao, C. F., Wang, Y., Shi, X. Q., Zhang, D. Z., Wang, C. Y., Jiang, J. H., Zhang, Q., and Fan, H.: Estimating the contribution of local primary emissions to particulate pollution using high-density station observations, J. Geophys. Res-Atm., 124, 2019.

Zhao, S., Yu, Y., Yin, D., Qin, D., He, J., and Dong, L.: Spatial patterns and temporal variations of six criteria air pollutants during 2015 to 2017 in the city clusters of Sichuan Basin, China, Sci. Total Environ., 624, 540-557, 2018.

Zhao, X., Zhao, P., Xu, J., Meng, W., Pu, W., Dong, F., He, D., and Shi, Q.: Analysis of a winter regional haze event and its formation mechanism in the North China Plain, Atmos. Chem. Phys., 13, 5685-5696, 2013a.

Zheng, G., Duan, F., Su, H., Ma, Y., Cheng, Y., Zheng, B., Zhang, Q., Huang, T., Kimoto, T., and Chang, D.: Exploring the severe winter haze in Beijing: the impact of synoptic weather, regional transport and heterogeneous reactions, Atmos. Chem. Phys., 15, 2969-2983, 2015.

Zhu, Y., Huang, L., Li, J., Ying, Q., Zhang, H., Liu, X., Liao, H., Li, N., Liu, Z., and Mao, Y.: Sources of particulate matter in China: Insights from source apportionment studies published in 1987–2017, Environ. Int., 115, 343-357, 2018.

Table 1. Predicted source-region contributions to $PM_{2.5}$ in the 18 SCB city centers in the winter.

Region ID	**City**	**$PM_{2.5}$**	**Contributions from each region, SOA, and others* (%)**													
		($\mu g\ m^{-3}$)	**R1**	**R2**	**R3**	**R4**	**R5**	**Within SCB**	**R6**	**R7**	**R8**	**R9**	**Outside SCB**	**SOA**	**Others**	**Non-local#**
R1	Chongqing$	191	**67.7**	4.5	3.7	0.4	1.8	**78.1**	2.7	11.1	0.1	0.9	**14.8**	3.9	3.3	**25.2**
R2	Bazhong	65	2.0	**42.6**	2.8	1.2	2.9	**51.5**	1.7	31.9	0.1	2.7	**36.4**	6.9	5.1	**45.3**
	Dazhou	89	2.4	**47.3**	1.7	0.5	7.5	**59.4**	1.5	27	0.1	1.6	**30.2**	6.0	4.3	**42.3**
	Guangan	109	8.9	**50.4**	2.0	0.5	5.4	**67.2**	2.3	19.6	0.1	1.4	**23.4**	5.8	3.5	**40.2**
	Guangyuan	60	2.3	**45.5**	5.2	1.8	1.7	**56.5**	1.3	25.5	0.1	4.2	**31.1**	6.5	5.8	**42.1**
	Nanchong	120	6.1	**56.5**	3.2	0.6	3.1	**69.5**	1.8	18.1	0.1	1.3	**21.3**	5.7	3.4	**34.3**
R3	Deyang	143	2.7	4.6	**58.0**	14.5	0.8	**80.6**	0.8	9.4	0.1	1.6	**11.9**	4.2	3.4	**34.5**
	Leshan	125	2.9	3.1	**58.7**	15.1	0.6	**80.4**	1.2	8.2	0.1	1.2	**10.7**	5.7	3.0	**32.4**
	Luzhou	149	13.9	4.8	**53.9**	1.8	1.2	**75.6**	3.8	11.2	0.1	1.0	**16.1**	5.4	2.9	**37.8**
	Meishan	153	2.5	3.1	**40.2**	36.3	0.6	**82.7**	0.9	7.7	0.1	1.1	**9.8**	4.6	2.9	**52.3**
	Mianyang	114	2.7	6.8	**60.3**	4.8	1.1	**75.7**	0.9	12.4	0.1	2.2	**15.6**	4.9	3.8	**31.0**
	Neijiang	140	11.3	7.6	**51.9**	2.8	1.3	**74.9**	2.4	12.7	0.1	1.1	**16.3**	5.6	3.1	**39.3**
	Suining	100	11.7	33.5	**14.4**	1.1	3.2	**63.9**	2.6	21.4	0.1	1.7	**25.8**	6.8	3.6	**75.3**
	Ya'an	79	3.2	3.6	**45.9**	20.1	0.7	**73.5**	1.4	11.0	0.3	2.3	**15.0**	7.6	3.8	**42.6**
	Yibin	134	6.8	4.1	**60.1**	5.5	0.9	**77.4**	2.8	9.7	0.1	1.1	**13.7**	6.0	3.0	**31.0**
	Zigong	145	8.9	6.0	**57.1**	3.2	1.1	**76.3**	2.4	11.4	0.1	1.1	**15.0**	5.5	3.3	**34.2**
	Ziyang	131	5.8	7.3	**54.0**	7.1	1.2	**75.4**	1.7	12.6	0.1	1.4	**15.8**	5.6	3.2	**37.2**
R4	Chengdu	144	2.2	3.5	20.4	**55.2**	0.6	**81.9**	0.8	8.2	0.1	1.4	**10.5**	4.2	3.5	**37.2**

* Others include initial and boundary conditions, windblown dust, and sea salt.

Non-local=Within SCB + Outside SCB – Local.

$ the city center of Chongqing.

Table 2. Predicted citywide area-weighted average $PM_{2.5}$ concentrations and source-region contributions in the 18 SCB cities in the winter and summer.

Region ID	No. of grid cells	Total area (km^2)	City	No. of grid cells	Total area (km^2)	Winter			Summer		
						$PM_{2.5}$ ($\mu g\ m^{-3}$)	Contributions (%)		$PM_{2.5}$ ($\mu g\ m^{-3}$)	Contributions (%)	
							Local	Non-local#		Local	Non-local #
R1	248	28011	Western Chongqing	248	28011	**99**	37.8	52.1	**27**	36.8	36.0
R2	543	56265	Bazhong	106	10734	**51**	27.9	58.2	**14**	19.3	43.6
			Dazhou	139	14689	**64**	29.1	58.6	**16**	21.6	45.7
			Guangan	60	5618	**100**	40.6	49.5	**23**	32.3	40.3
			Guangyuan	133	14182	**50**	28.3	57.1	**13**	23.4	40.5
			Nanchong	105	11042	**89**	47.9	41.4	**20**	36.3	34.1
R3	998	98185	Deyang	59	5346	**101**	49.9	40.2	**25**	44.5	32.8
			Leshan	107	11599	**81**	42.5	44.4	**14**	35.0	29.7
			Luzhou	112	10758	**92**	35.3	53.8	**20**	25.6	43.7
			Meishan	74	6570	**120**	42.6	47.7	**26**	36.7	35.8
			Mianyang	171	18012	**59**	36.8	49.2	**15**	32.9	36.7
			Neijiang	58	4859	**122**	45.8	44.8	**29**	40.8	34.7
			Suining	50	4743	**104**	30.3	59.7	**23**	25.4	48.4
			Ya'an	131	13493	**45**	34.5	49.2	**6**	27.9	35.1
			Yibin	117	11827	**101**	50.1	39.1	**21**	43.3	24.9
			Zigong	45	3935	**126**	51.3	39.4	**30**	47.3	26.9
			Ziyang	74	7042	**115**	40.3	50.2	**25**	32.6	41.9
R4	105	10753	Chengdu	105	10753	**110**	46.5	44.1	**31**	44.6	33.0
R5	390	44371	Eastern Chongqing	390	44371	**54**	21.0	66.0	**15**	14.7	52.1

Non-local =100%-Local-SOA-Others; Others include initial and boundary conditions, windblown dust, and sea salt.

Table 3. Predicted maximum daily contribution from a given region (MDCs) in the SCB city center and the corresponding $PM_{2.5}$ concentrations in the city center on the same day. Only winter data are included in this table. The units are μg m^{-3}. The numbers in the bold present the contributions due to local emissions or that from R7.

Region ID	**Cities**	**MDCs (total $PM_{2.5}$ concentrations)**										
		Within SCB				**Outside SCB**					**SOA**	**Others**[#]
		R1	**R2**	**R3**	**R4**	**R5**	**R6**	**R7**	**R8**	**R9**		
R1	Chongqing[$]	**291 (353)**	54 (414)	48 (294)	16 (302)	15 (143)	22 (290)	**99 (200)**	1 (182)	8 (212)	12 (160)	12 (294)
R2	Bazhong	8 (160)	**83 (139)**	23 (160)	18 (160)	7 (64)	14 (68)	**73 (109)**	0 (140)	6 (90)	14 (327)	11 (34)
	Dazhou	46 (219)	**123 (216)**	16 (171)	6 (171)	34 (219)	12 (77)	**79 (190)**	0 (173)	5 (54)	18 (367)	8 (54)
	Guangan	72 (159)	**129 (205)**	31 (180)	10 (180)	22 (225)	14 (102)	**76 (165)**	0 (234)	5 (129)	16 (219)	7 (75)
	Guangyuan	11 (122)	**60 (107)**	35 (122)	15 (122)	4 (56)	10 (86)	**62 (100)**	0 (91)	11 (46)	16 (226)	10 (25)
	Nanchong	58 (180)	**152 (242)**	50 (200)	12 (243)	18 (238)	13 (141)	**78 (166)**	0 (177)	5 (136)	17 (178)	10 (71)
R3	Deyang	32 (226)	30 (257)	**170 (296)**	147 (288)	4 (257)	14 (215)	**70 (132)**	0 (215)	9 (137)	13 (91)	10 (67)
	Leshan	15 (270)	15 (166)	**163 (270)**	57 (222)	4 (166)	10 (222)	**47 (122)**	1 (108)	5 (118)	15 (222)	9 (105)
	Luzhou	115 (245)	33 (207)	**211 (261)**	21 (240)	10 (207)	18 (259)	**71 (272)**	1 (192)	6 (90)	17 (307)	10 (182)
	Meishan	17 (189)	22 (379)	**155 (379)**	138 (235)	4 (176)	11 (263)	**54 (263)**	1 (379)	5 (80)	15 (164)	9 (100)
	Mianyang	24 (209)	30 (170)	**219 (294)**	67 (305)	6 (168)	11 (144)	**70 (112)**	0 (337)	9 (86)	16 (294)	11 (46)
	Neijiang	93 (214)	39 (168)	**161 (205)**	49 (309)	6 (168)	17 (165)	**79 (198)**	1 (192)	5 (198)	19 (181)	9 (164)
	Suining	75 (183)	110 (242)	**105 (186)**	25 (225)	14 (210)	17 (151)	**83 (167)**	0 (154)	5 (79)	17 (198)	10 (41)
	Ya'an	14 (126)	17 (205)	**79 (170)**	88 (234)	3 (205)	8 (170)	**35 (205)**	1 (123)	6 (40)	15 (189)	9 (43)
	Yibin	74 (283)	21 (162)	**160 (217)**	45 (164)	5 (236)	16 (188)	**58 (166)**	1 (122)	4 (147)	14 (170)	9 (127)
	Zigong	64 (281)	34 (171)	**162 (214)**	51 (291)	6 (171)	17 (192)	**71 (195)**	1 (195)	5 (199)	16 (283)	10 (162)
	Ziyang	39 (192)	33 (137)	**164 (298)**	63 (176)	7 (120)	19 (181)	**73 (155)**	1 (298)	6 (176)	18 (203)	9 (126)
R4	Chengdu	16 (232)	23 (225)	86 (267)	**250 (327)**	4 (139)	11 (267)	**63 (151)**	1 (166)	7 (132)	16 (228)	9 (101)

[#] Others include initial and boundary conditions, windblown dust, and sea salt.

[$] includes the city center of Chongqing.

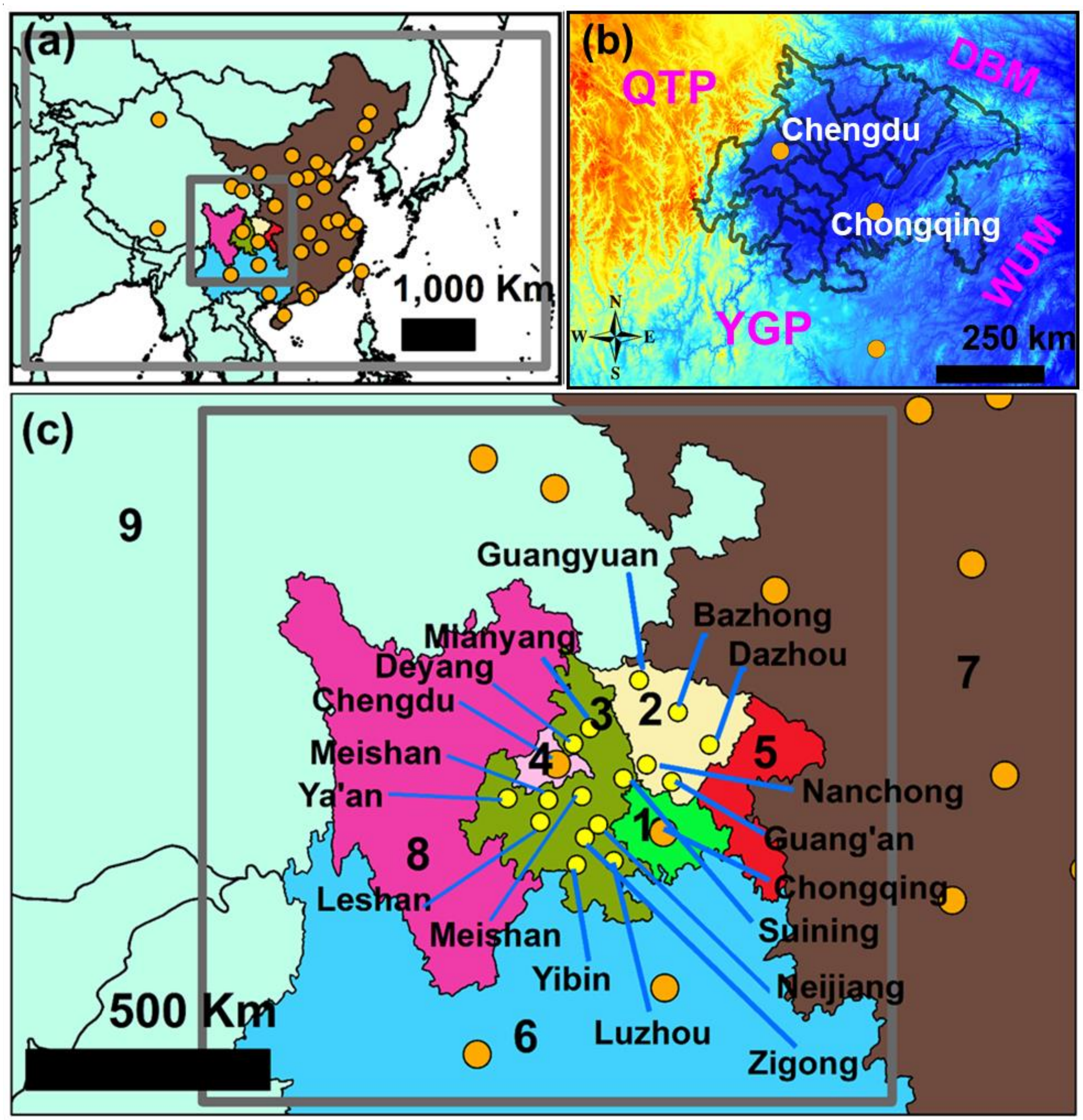

Figure 1. (a) Locations of the 12-km and 36-km domains (grey rectangles) and the locations of provincial capitals and municipalities (orange circles), (b) terrain within and surrounding the 18 cities of the SCB (black line), and (c) locations of region categories 1~9 and the prefecture-level cities (yellow circles). Regions 1~5 are the cities within the SCB. Regions 1, 4, and 5 are western Chongqing, Chengdu, and eastern Chongqing, respectively. The city center of Chongqing is located in western Chongqing. Region 8 is the area of Sichuan Province excluding those cities in the SCB. QTP, Qinghai-Tibetan Plateau; YGP, Yunnan-Guizhou Plateau; DBM, Dabashan Mountains; WUM, Wushan Mountains.

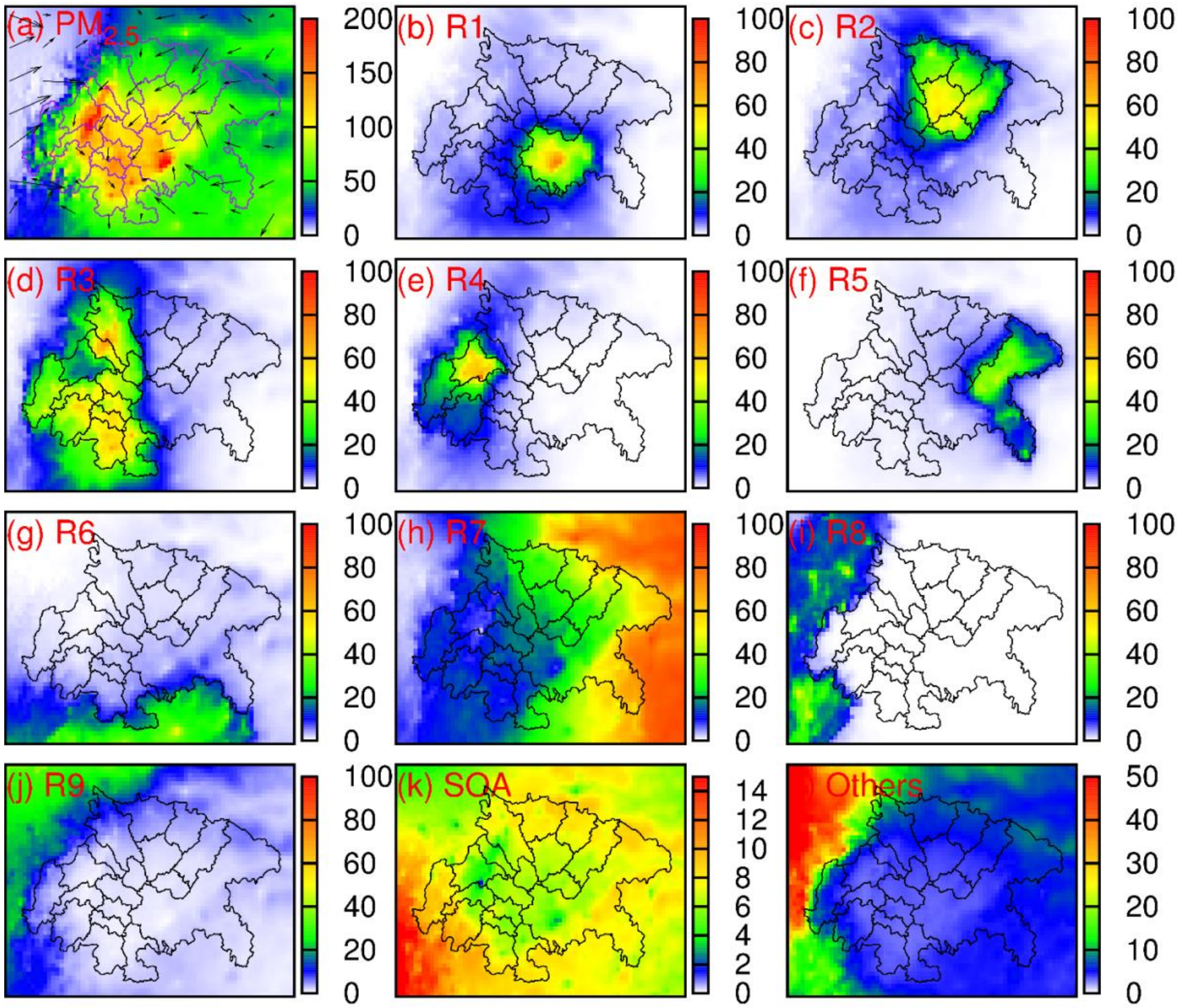

Figure 2. (a) Spatial distributions of predicted $PM_{2.5}$ concentrations (μg m^{-3}) and (b-l) source-region contributions to $PM_{2.5}$ (%) in the winter. Others include IC, BC, windblown dust, and sea salt. Black arrows in (a) are wind vectors.

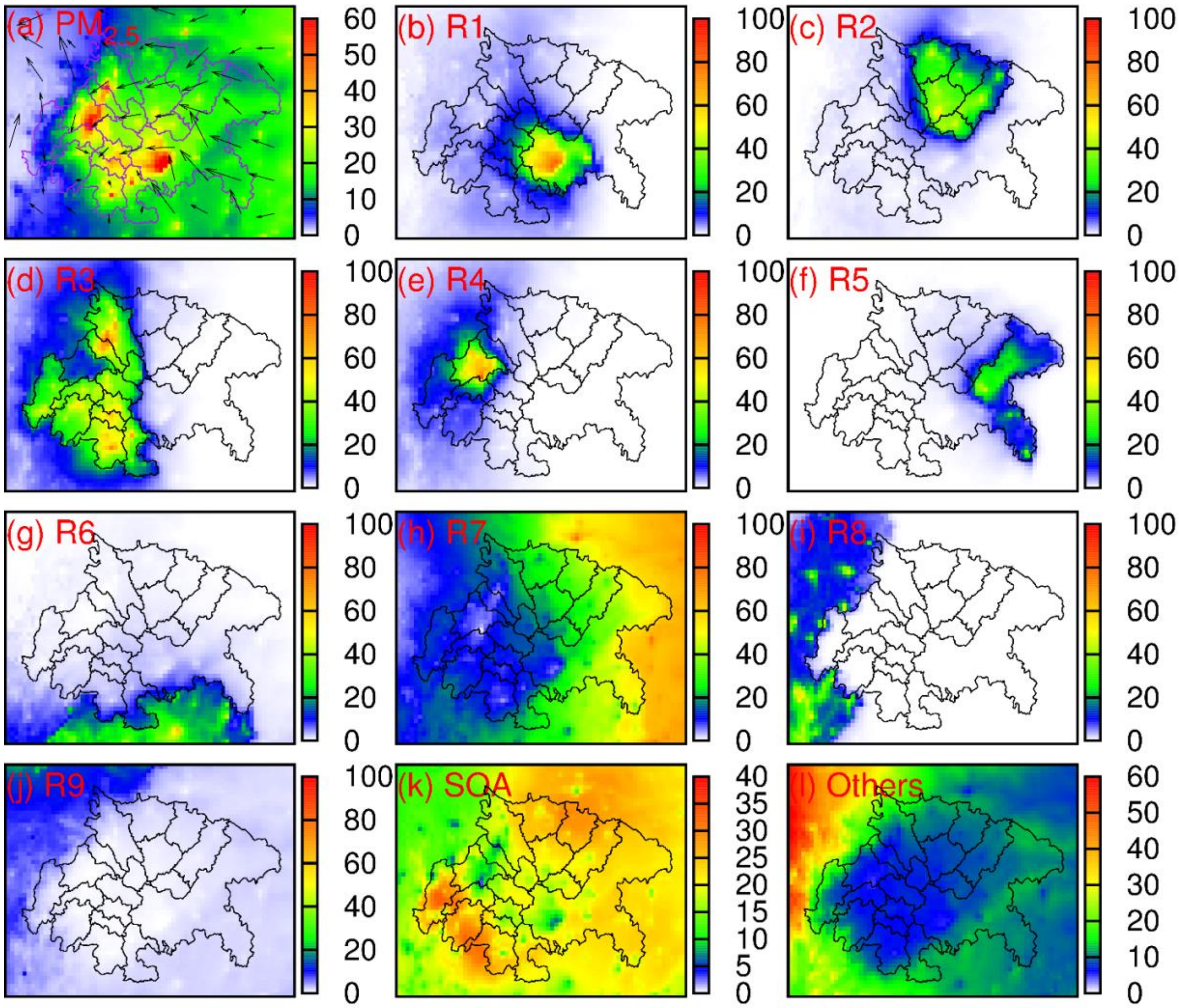

Figure 3. (a) Spatial distributions of predicted $PM_{2.5}$ concentrations (μg m^{-3}) and (b-l) the source-region contributions to $PM_{2.5}$ (%) in the summer. Others include IC, BC, windblown dust, and sea salt.

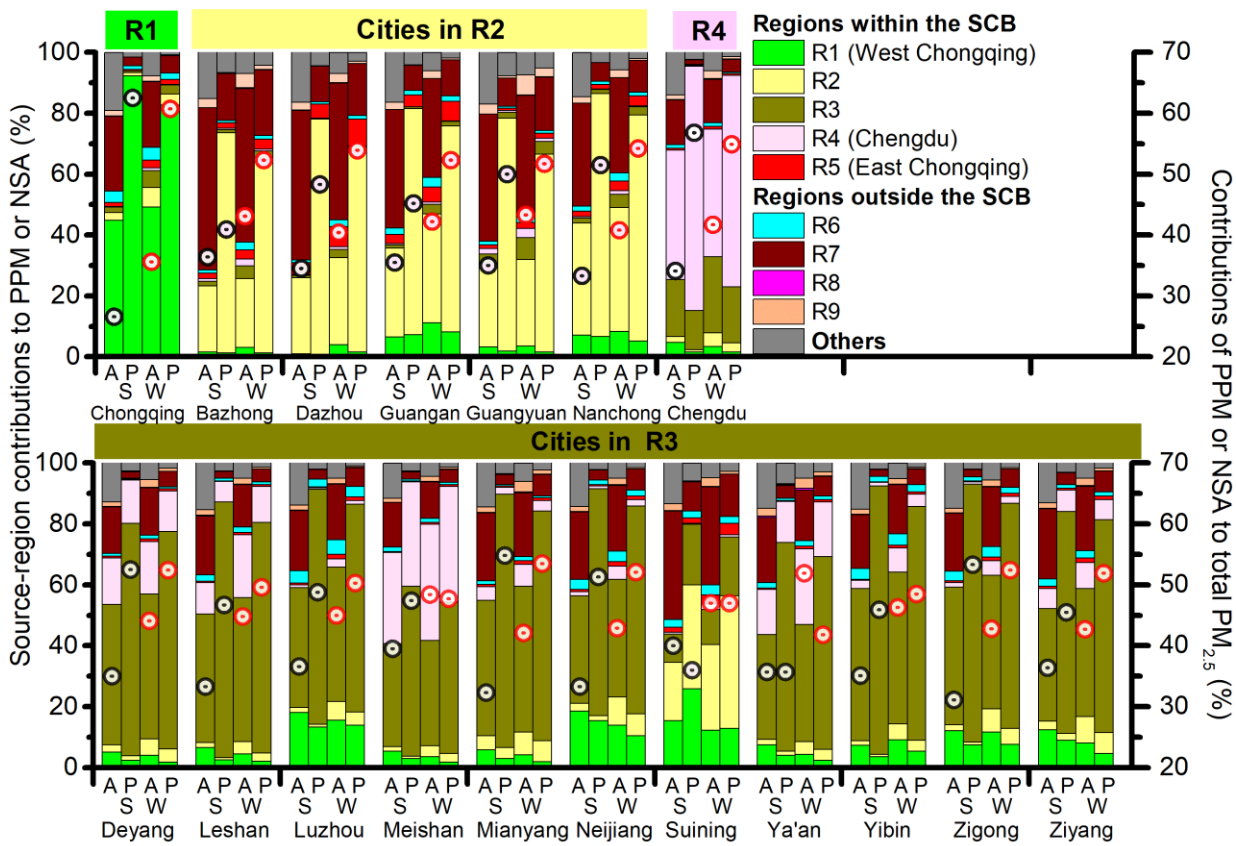

Figure 4. Predicted source-region contributions to SIA (A) and PPM (P) (bars, left y-axis) and the predicted proportions of SIA and PPM in $PM_{2.5}$ (circles, right y-axis) for the 18 city centers of the SCB in the summer (S) and winter (W). Others include IC, BC, windblown dust, and sea salt.